

Digital Twin-Based Network Management for Better QoE in Multicast Short Video Streaming

Xinyu Huang, *Student Member, IEEE*, Shisheng Hu, *Student Member, IEEE*, Haojun Yang, *Member, IEEE*,
Xinghan Wang, *Student Member, IEEE*, Yingying Pei, *Student Member, IEEE*,
and Xuemin (Sherman) Shen, *Fellow, IEEE*

Abstract—Multicast short video streaming can enhance bandwidth utilization by enabling simultaneous video transmission to multiple users over shared wireless channels. The existing network management schemes mainly rely on the sequential buffering principle and general quality of experience (QoE) model, which may deteriorate QoE when users' swipe behaviors exhibit distinct spatiotemporal variation. In this paper, we propose a digital twin (DT)-based network management scheme to enhance QoE. Firstly, user status emulated by the DT is utilized to estimate the transmission capabilities and watching probability distributions of sub-multicast groups (SMGs) for an adaptive segment buffering. The SMGs' buffers are aligned to the unique virtual buffers managed by the DT for a fine-grained buffer update. Then, a multicast QoE model consisting of rebuffering time, video quality, and quality variation is developed, by considering the mutual influence of segment buffering among SMGs. Finally, a joint optimization problem of segment version selection and slot division is formulated to maximize QoE. To efficiently solve the problem, a data-model-driven algorithm is proposed by integrating a convex optimization method and a deep reinforcement learning algorithm. Simulation results based on the real-world dataset demonstrate that the proposed DT-based network management scheme outperforms benchmark schemes in terms of QoE improvement.

Index Terms—Digital twin, network management, multicast transmission, short video, QoE.

I. INTRODUCTION

SHORT video platforms such as TikTok, Instagram Reels, and YouTube Shorts have experienced a dramatic surge in user scale, with TikTok's monthly active users reaching 1.7 billion in 2023 [1]. Seamless video requests bring a huge traffic and computing burden to communication networks, which cause frequent playback lags and video quality fluctuation, especially in areas with high user density, thereby deteriorating users' watching experience [2]. Multicast transmission, as an essential technology in wireless networks, can enable a single data stream to be disseminated to numerous users in a group simultaneously. By multicasting short videos to the users with similar characteristics and geographical locations, the redundancy in video rendering, transcoding, and transmission can be effectively reduced, thereby alleviating the network traffic and computing burden [3].

For multicast short video streaming (MSVS) services, one of the key metrics to evaluate the performance is quality of

experience (QoE). It is typically a multi-dimensional metric used to quantify users' subjective and objective watching experience [4]. For instance, video quality (resolution, bitrate), latency, as well as rebuffering events are the most important factors that dominate the QoE level [5]. To maintain users' QoE at a high level, efficient network management is essential, such as buffer management and resource scheduling [6], [7]. Specifically, due to the limited bandwidth and computing resources, it needs to be determined which versions and quantities of segments (sequential components of a video sequence) should be transmitted to users' buffers, and at what priority levels. Furthermore, due to asynchronous swipe behaviors in one multicast group (MG), one MG can be further divided into multiple sub-MGs (SMGs). The SMG with a leading video playback is defined as the leading SMG, otherwise, the lagging SMG. The bandwidth and computing resources need to be flexibly and accurately assigned to each SMG to reduce service delay. Nevertheless, existing network management schemes are mainly based on the sequential buffering principle and general QoE model while neglecting the impact of users' swipe behaviors and the mutual influence of SMGs' segment buffering. As a result, users may suffer from frequent playback lags and low video quality, thus leading to a low QoE.

Digital twin (DT) is a promising technique to optimize network management for better QoE. DT is defined as a full digital representation of a physical object, and real-time synchronization between the physical object and its corresponding digital replica [8]. As an essential component embedded in the next-generation communication networks, DT is comprised of a data pool as well as several data processing and decision-making modules, which can efficiently emulate users' behaviors and network conditions, abstract distilled features, and make network management decisions [9], [10]. Owing to its powerful emulation, analysis, and decision-making capabilities, communication networks can more intelligently perceive SMGs' behavior patterns, finely control SMGs' buffer update, and provide customized network management strategies to enhance users' QoE. In this work, the precise role of constructed DT is to emulate users' future network conditions and swipe behaviors, abstract the watching probability distribution of segments, and make tailored network management decisions based on the emulated user status and abstracted information.

The motivation of the DT-based network management for MSVS includes three aspects. Firstly, due to users' stochastic swipe behaviors, users' viewing sequences are usually non-sequential. The existing sequential buffering principle can

Xinyu Huang, Shisheng Hu, Haojun Yang, Xinghan Wang, Yingying Pei, and Xuemin (Sherman) Shen are with the Department of Electrical and Computer Engineering, University of Waterloo, Waterloo, ON N2L 3G1, Canada (E-mail: {x357huan, s97hu, h88yang, x243wang, y32pei, sshen}@uwaterloo.ca).

cause the segments to be swiped to not being buffered in time, resulting in playback lags. Moreover, users' buffer lengths are usually overestimated due to multicast segment buffering, which can bring inaccurate rebuffering time estimation. Therefore, it is essential to develop an efficient segment buffering scheme that adapts well to users' swipe behaviors. Secondly, the QoE model is typically composed of multiple factors. Due to the impact of multicast transmission and segment buffering priority, different QoE factors among SMGs influence each other, collectively impacting the MG's QoE. Therefore, it is paramount to establish a QoE model specifically tailored for MSVS. Thirdly, since network management is usually a multi-variable decision-making problem, such as the segment version selection and resource scheduling, the interplay among the variables makes the optimization problem complex and difficult to solve. Therefore, how to design an efficient algorithm to solve it for users' high QoE is important.

Designing an efficient DT-based network management scheme needs to address the following challenges: 1) incorporating the impact of users' swipe behaviors in multicast segment buffering; 2) establishing an accurate multicast QoE model; 3) designing an efficient algorithm to solve the complex multi-variable decision-making problem. Specifically, users' swipe behaviors are stochastic and spatiotemporally varied, which are difficult to accurately predict in real time. Therefore, how to conduct effective data abstraction to obtain the distilled swipe feature and utilize it to facilitate accurate multicast segment buffering is challenging. Furthermore, since the lagging SMG can still receive segments from other leading SMGs in its scheduling slot, this interactivity results in complex QoE estimation. Therefore, how to characterize the impact of multicast segment buffering among SMGs on the QoE model is challenging. Finally, since the network management problem is usually a mixed-integer non-convex problem, directly using model-based or data-driven algorithms can lead to a loss in the system performance. Therefore, how to ingeniously combine the advantages of model-based and data-driven algorithms to efficiently solve the formulated problem is challenging.

In this paper, we propose a DT-based network management scheme, which can effectively enhance users' QoE. The main contributions are summarized as follows:

- Firstly, we propose a novel DT-assisted buffer management scheme to incorporate the impact of swipe behaviors. Specifically, users' historical status, including locations, channel conditions, preferences and swipe timestamps, is stored in the DT for status emulation. The emulated status is used to abstract the SMGs' transmission capabilities and the watching probability distribution of segments. Based on the abstracted information, DT can make an adaptive segment buffering decision. Furthermore, DT is utilized to construct and manage virtual buffers for each SMG for a fine-grained buffer update.
- Secondly, we establish a multicast QoE model to quantify the impact of multicast segment buffering among SMGs. Specifically, the multicast QoE model is built as a weighted sum of rebuffering time, video quality, and quality variation, where the weighting factors are the integration of buffering order and users' sensitivity

degrees. The rebuffering time estimation relies on the multicast transmission delay as well as the parallel transmission and transcoding process. The video quality and quality variation depend on the relationship between the segment version and structural similarity index measure (SSIM). Based on these elements, an accurate multicast QoE model is established.

- Thirdly, we formulate a joint optimization problem of segment version selection and slot division to maximize QoE. Since the formulated problem is a mixed-integer nonlinear programming problem, it is hard to directly use a model-based or data-driven algorithm to solve it. Therefore, we propose a data-model-driven algorithm. Specifically, a convex optimization method is embedded in a deep reinforcement learning (DRL) algorithm to decouple the joint optimization problem and reduce the action dimension, which can efficiently solve the formulated problem. The extensive simulation results on real-world short video streaming datasets show that the proposed DT-based network management scheme can effectively enhance QoE as compared with the state-of-the-art network management schemes.

The remainder of this paper is organized as follows. Related works are introduced in Section II. The system model is first built in Section III. Then, the DT-assisted buffer management and the multicast QoE model are presented in Sections IV and V, respectively. Next, the problem formulation and the proposed scheduling algorithm are shown in Section VI, followed by simulation results in Section VII. Finally, Section VIII concludes this paper.

II. RELATED WORK

To facilitate the efficient MSVS within radio access networks (RANs), extensive works are devoted to optimizing network management performance from different directions, such as adaptive video bitrate, multi-connectivity management, and transmission and transcoding scheduling. Specifically, Taha *et al.* studied the impact of the characteristics of videos, wireless channel capabilities, and users' profiles on the MG's QoE, and designed an efficient machine learning algorithm to adaptively adjust the video bitrate [11]. Lie *et al.* integrated the scalable video coding (SVC) technology with the transmission delay constraint, and exploited the hard deadline constrained prioritized data structure and user feedback to make an optimal adaptive encoding and scheduling strategy, which can enhance the average network throughput [12]. To achieve high-quality and cost-efficient multicast video services, Zhong *et al.* proposed a novel buffer-nadir-based multicast mechanism, formulated the multicast-aware task offloading problem, and devised a joint optimization algorithm for data scheduling and task offloading, respectively [13]. Additionally, Zuhra *et al.* proposed the procedures of establishing multi-connectivity and a greedy approximation algorithm to solve the associated resource allocation problem, which can effectively increase the number of served users [14]. Daher *et al.* proposed a dynamic clustering algorithm based on the minimization of a submodular function that integrated the traffic in each cell and the MG's

average signal to interference plus noise ratio (SINR), which can maintain an acceptable transmission failure probability and enhance the MG's average SINR [15]. To improve the robustness of multicast transmission, Zhang *et al.* proposed a cooperative multicast framework, where users can recover videos with quality proportional to their channel conditions. A joint power allocation and segment scheduling problem was formulated to minimize the overall distortion and solved by a provably convergent optimal algorithm [16]. Considering the characteristic of stochastic channels, Zhang *et al.* further analyzed the video-layer recovery failure probability and estimated the MG's average QoE. Based on the information, an optimal scheduling algorithm was developed based on the hidden monotonicity of the problem to maximize the MG's QoE [17]. However, these schemes usually require real-time data collection and efficient data processing on user and network status information, which poses a high requirement for efficient network management.

As an essential virtualization technology, DT was first introduced to monitor and mitigate anomalous events for flying vehicles [18]. By introducing DT into RANs, we can realize holistic network virtualization for efficient network management. We refer readers to recent comprehensive surveys and tutorials on DT to become familiar with this topic [19]–[21]. There also exist some technical papers aiming at utilizing DT to improve network management performance. Specifically, Bellavista *et al.* proposed an application-driven DT networking middleware to simplify the interaction with heterogeneous distributed industrial devices and flexibly manage network resources, which can effectively reduce communication overhead [22]. Qi *et al.* leveraged the DT as a centric controller to encourage edge devices to share their idle resources and get a reward from other devices with poor network performance, which can efficiently reduce the service delay [23]. Considering that the real networks are not static, Dong *et al.* constructed the DT of the wireless networks to generate labeled training samples, where the network topology, channel and queueing models, and fundamental rules were adopted in the DT to mirror the real networks [24]. A DT-assisted resource demand prediction scheme was proposed to enhance prediction accuracy for MSVS, including the DT construction, the accurate and fast MG construction, and the MG's swipe probability distribution abstraction [25]. To further enhance users' QoE in dynamic and heterogeneous environments, an intelligent resource allocation strategy with low communication overhead was proposed, where DT was utilized to monitor the current network operation status and enable intelligent decision-making [26]. Furthermore, Jeremiah *et al.* proposed to construct a central DT to simulate dynamic and heterogeneous networks, which can enhance the efficiency of edge collaboration and real-time resource information availability [27]. These pioneering works can effectively improve network management performance in terms of communication overhead, service delay, and QoE.

Compared with related network management work, we have proposed a novel DT-assisted buffer management scheme to incorporate the impact of swipe behaviors. Furthermore, we have established a multicast QoE model to quantify the impact

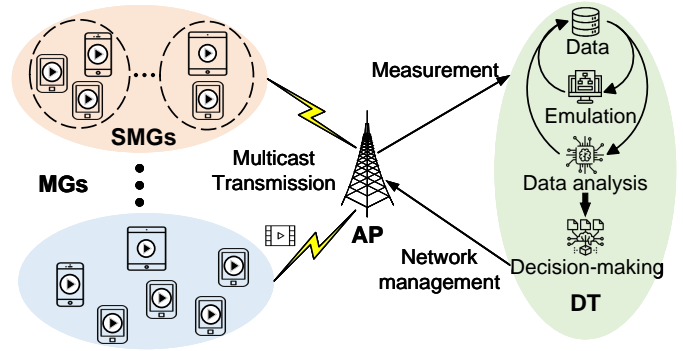


Fig. 1. DT-assisted MSVS framework.

of multicast segment buffering among SMGs. Finally, a data-model-driven algorithm has been developed to efficiently solve the formulated mixed-integer nonlinear programming problem for better QoE.

III. SYSTEM MODEL

As shown in Fig. 1, we consider a DT-assisted MSVS scenario, which consists of an access point (AP), multiple MGs, and one DT.

- **Access point:** The AP owns communication, computing, and caching capabilities. Based on users' requests, cached video sequences will be transcoded to appropriate bitrates and then transmitted to each MG. In addition, it is responsible for collecting users' network-related and behavior-related information to update DT data.
- **Multicast group:** Each MG consists of multiple users using short video services. The same video sequences will be transmitted from the AP to one MG over shared wireless channels. The MG's construction and update mainly depend on users' similarities in swipe behaviors, channel conditions, locations, and preferences, as discussed in [3]. Due to asynchronous swipe behaviors, users' devices in the same MG still have different playback stamps and buffer lengths. Therefore, one MG is further divided into multiple SMGs, denoted by $\mathcal{G} = \{1, \dots, G\}$. The number of total users in the system is denoted by K . The set of users in SMG g is denoted by $\{\mathcal{K}_g\}_{g \in \mathcal{G}}$.
- **Digital twin:** It consists of a database storing users' status information, a status emulation module, as well as multiple data analysis and decision-making modules. DT data comes from two aspects, i.e., data measurement and emulation module. The former is used to obtain the label data to detect whether the emulated data is accurate enough and supplement DT data when emulated data has a large deviation. The latter uses machine learning-based algorithms to predict users' future status. The data analysis module is responsible for abstracting distilled data features, such as swipe probability distribution, request density, user satisfaction, etc, which can facilitate tailored network management in the decision-making module.

As shown in Fig. 2, we present the proposed DT-assisted MSVS workflow. Specifically, the user status emulation module can generate user status information. When the generated

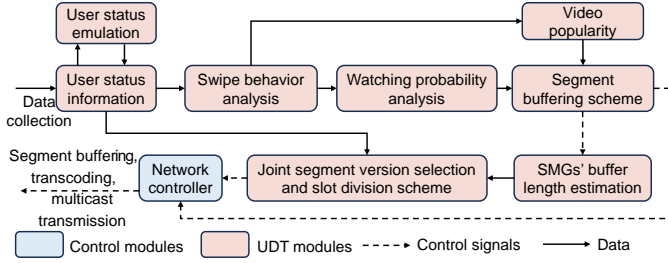


Fig. 2. Proposed DT-assisted MSVS workflow.

data has a significant deviation from the actual user status data, new actual data is collected to correct user status information. The user status information is first utilized to abstract the user's swipe feature, such as swipe probability distribution, which can update the video popularity and watching probability distribution of segments. The updated information is then used to make the tailored segment buffering and SMGs' buffer update decisions. Next, SMGs' buffer lengths are estimated, which are integrated with user status information to make a joint segment version selection and slot division decision. Finally, all network management decisions are transferred to the network controller to guide the physical entities to implement.

IV. DT-ASSISTED BUFFER MANAGEMENT SCHEME

In this section, we first propose an adaptive segment buffering scheme based on the DT-analyzed watching probability distribution, and then design a fine-grained buffer update scheme based on the DT-assisted virtual buffer management.

A. DT Construction

DT consists of multiple modules, which are summarized as status emulation, data analysis, and decision-making, as shown in Fig. 2.

Firstly, since network conditions and user behaviors are essential to reflect users' characteristics and requirements, we utilize the AP to collect users' data from two aspects, i.e., networking-related data and behavior-related data. The networking-related data include users' channel conditions and locations, which are utilized to estimate the transmission capabilities. The behavior-related data consist of users' swipe timestamps and preferences. The long short-term memory (LSTM) method is utilized to mine data correlation, which can effectively emulate users' future networking-related data and behavior-related data. This operation can effectively reduce frequent data interaction costs between DT and users. By integrating these two kinds of data, DT can accurately emulate users' real-time status for network management.

Secondly, two kinds of data analysis modules are embedded in the DT, i.e., the swipe behavior analysis module and the watching probability analysis module. The former has been investigated in [3] for resource demand prediction. The latter is our focus in this paper, which aims at assisting the buffer management. Specifically, due to the impact of sequential playback and swipe behaviors, each segment's watching probability

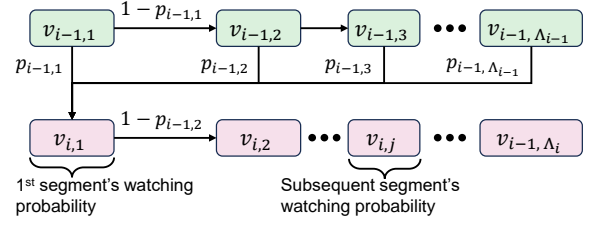


Fig. 3. Watching probability analysis.

has a dependable relationship. From the aspects of the first and subsequent segments' swipe probabilities, the watching probability distribution of segments is derived in DT. Based on the derived information, DT can realize an accurate buffer management.

Thirdly, based on the emulated status and analyzed data, DT can realize tailored decision-makings to further enhance users' QoE. Three kinds of decision-making modules are designed to make the segment buffering scheme, the SMGs' buffer update scheme, and the joint segment version selection and slot division scheme, respectively. These modules are intricately coupled, where the output of one module seamlessly transitions into the input of the following module, collectively influencing QoE. A data-model-driven algorithm is proposed to decouple the joint optimization problem and reduce the action dimension for efficient network management.

B. DT-Assisted Segment Buffering Scheme

Due to users' diversified swipe behaviors, the segments to be watched do not follow a sequential order, which can cause different watching probabilities. To reduce rebuffering events, we need to analyze which segments should be prioritized for buffering. Therefore, we design a DT-assisted segment buffering scheme. The specific analysis is as follows.

As shown in Fig. 3, DT recommends a video list for the MG in each large timescale, referred in [3]. Each video sequence consists of multiple segments with the same time length. The recommended video list is denoted by $\{v_{i,j}\}_{i \in \mathcal{N}, j \in \{1, \dots, \Lambda_i\}}$, where \mathcal{N} is the recommended video index list, and Λ_i is the number of segments in video i . The watching probability distribution of segments has a dependable relationship [28]. Let $w_{i,j}$ represent the watching probability of segment $v_{i,j}$. For any two successive segments j and $j+1$ in video i , the watching probability of segment $j+1$ is derived as

$$w_{i,j+1} = w_{i,j}(1 - p_{i,j}), \forall i \in \mathcal{N}, j \in \{1, \dots, \Lambda_i - 1\}, \quad (1)$$

where $p_{i,j}$ is the swipe probability of segment $v_{i,j}$. Based on Eq. (1), we further analyze the watching probability distribution from the perspectives of 1st and subsequent segments.

For the 1st segment of video i , its watching probability is related to the swipe probability of all segments in previous video $i-1$. Therefore, the corresponding watching probability, $w_{i,1}$, is expressed as

$$w_{i,1} = w_{i-1,1} \left(p_{i-1,1} + \sum_{j=1}^{\Lambda_{i-1}-1} p_{i-1,j+1} \prod_{k=1}^j (1 - p_{i-1,k}) \right). \quad (2)$$

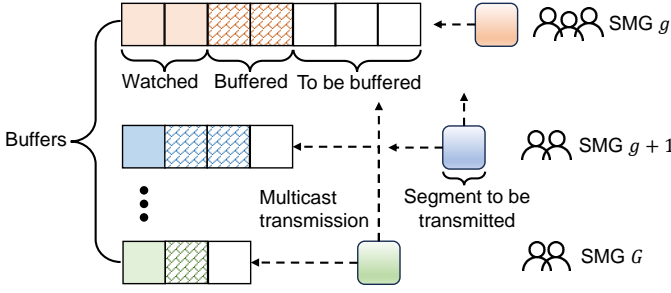


Fig. 4. Multicast transmission mechanism among SMG groups.

For the subsequent segment j of video i , its watching probability is only related to the swipe probability of previous segment $j - 1$. Therefore, the corresponding watching probability, $w_{i,j}$, is given by

$$w_{i,j} = w_{i,1} \prod_{k=1}^{j-1} (1 - p_{i,k}), \forall j \in \{2, \dots, \Lambda_i\}. \quad (3)$$

Based on the watching probability distribution, we can determine the segment buffering order from high to low. Furthermore, we analyze how many segments should be added to the MG's buffer in each scheduling slot, which needs to satisfy two requirements, i.e., 1) buffer requirement: buffer minimum segments to avoid buffer length empty; 2) resource requirement: assign all bandwidth and computing resources to each SMG to observe how many segments can be buffered.

For the buffer requirement, we need to guarantee the buffer length is larger than the scheduling slot length for each SMG. Therefore, we can have

$$n_{\text{buffer}} = \sum_{g \in \mathcal{G}} \left[\frac{T_s - q_g}{\tau} \right]^+, \quad (4)$$

where T_s and τ represent the scheduling slot length and the segment length, respectively. Here, q_g represents SMG g 's buffer length for current watching video sequence and function $[x]^+ = \max\{x, 0\}$, respectively.

For the resource requirement, we analyze the multicast transmission mechanism among SMG groups, as shown in Fig. 4. Each video sequence consists of multiple segments, represented by different colors. The index orders of SMGs are consistent with the video viewing positions, sorted from low to high. Since video playback is continuous, the segment to be transmitted to SMG $g + 1$'s buffer can also be transmitted to SMG g 's buffer to reduce repeated video transmission. Therefore, the transmission capability of SMG $g + 1$ needs to consider users' channel conditions both from itself and SMG g . Based on the above analysis, the maximum buffered segments within all reserved bandwidth and computing resources need to satisfy the following requirements, i.e.,

$$\begin{cases} \sum_{m=1}^{\tilde{n}_g^B} \sum_{l=1}^{\bar{l}} z_{g,m}^l \leq \min_{k \in \cup_{d=1}^g \mathcal{K}_d} T_s r_{g,k} \leq \sum_{m=1}^{\tilde{n}_g^B+1} \sum_{l=1}^{\bar{l}} z_{g,m}^l, \forall g \in \mathcal{G}, \\ \mu \sum_{m=1}^{\tilde{n}_g^C} \sum_{l=2}^{\bar{l}} z_{g,m}^l \leq T_s C \leq \mu \sum_{m=1}^{\tilde{n}_g^C+1} \sum_{l=2}^{\bar{l}} z_{g,m}^l, \forall g \in \mathcal{G}, \end{cases} \quad (5)$$

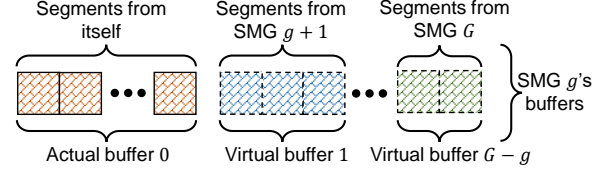


Fig. 5. DT-assisted SMG's buffer management.

where $z_{g,m}^l$ is the file size of segment m of version l for SMG g , which adopts the SVC principle [29]. Here, \tilde{n}_g^B and \tilde{n}_g^C represent the segment buffering numbers by allocating reserved bandwidth resources and computing resources, respectively. Here, \bar{l} is the average segment version and parameter μ is the computing density for segment transcoding. Here, C is the computing capacity of AP. Furthermore, $r_{g,k}$ is the data rate for user k in SMG g , which is given by

$$r_{g,k} = B \log_2 \left(1 + \frac{|h_{g,k}|^2 P_D}{N_0} \right), \quad (6)$$

where $h_{g,k}$ is the channel gain of user k in SMG g and N_0 is the noise power. Here, P_D and B represent the downlink transmission power and the reserved bandwidth resources for the MG, respectively.

Since Eq. (5) consists of monotonically increasing functions, the maximum segment buffering numbers \tilde{n}_g^B and \tilde{n}_g^C can be uniquely determined by increasing their own values. To satisfy both bandwidth and computing resource requirements, we select the smaller one between \tilde{n}_g^B and \tilde{n}_g^C as the segment buffering number, i.e., $\tilde{n}_g = \min\{\tilde{n}_g^B, \tilde{n}_g^C\}$. For one MG, the segment buffering number in the resource requirement is the maximum value of all SMGs' segment buffering numbers, i.e., $n_{\text{resource}} = \max_{g \in \mathcal{G}} \tilde{n}_g$.

According to the buffer and resource requirements, we can determine the segment buffering number, i.e., $n = \lfloor \max\{n_{\text{buffer}}, n_{\text{resource}}\} \rfloor$, where $\lfloor \cdot \rfloor$ is the floor operation. Then, the buffered segment sequence of SMG g can be obtained by integrating segment buffering number and order, denoted by Ω_g .

C. DT-Assisted Buffer Update Scheme

As shown in Fig. 5, we utilize the virtualization technology of DT to construct multiple virtual buffers for SMG g , where each virtual buffer corresponds to the divided and subsequent SMG's buffer. The buffer index of SMG g is denoted by f , ranging from 0 to $G - g$. In each time slot t , SMG g 's buffers are updated as

$$q_{g,t+1}^f = \begin{cases} \left[q_{g,t}^f - T_s + \tau |\Omega_g| \right]^+, & f = 0, \\ q_{g,t}^f + \tau |\Omega_{g+f}|, & \forall f \in [1, G - g], \end{cases} \quad (7)$$

where $|\Omega_g|$ is the segment buffering number of SMG g .

When SMG g starts to watch the next video, the current buffers 0 to $G - 1$ will be replaced by new buffers 1 to G , and a new empty virtual buffer will be added as buffer G . Assuming that within each scheduling slot, the number

of swipe behaviors for each SMG is at most once. An indicator function $\mathbb{S}_{g,t}$ is introduced, where $\mathbb{S}_{g,t} = 1$ denotes a swipe behavior and $\mathbb{S}_{g,t} = 0$ denotes no swipe behavior. By integrating the impact of swipe behaviors, SMG g 's buffer update can be further modified as

$$\tilde{q}_{g,t+1}^f = \begin{cases} q_{g,t+1}^f, & \mathbb{S}_{g,t} = 0, \\ q_{g,t+1}^{f+1}, & \mathbb{S}_{g,t} = 1 \ \& \ f \in [0, G - g - 1], \\ 0, & \mathbb{S}_{g,t} = 1 \ \& \ f = G - g. \end{cases} \quad (8)$$

V. MULTICAST QOE MODEL ESTABLISHMENT

To evaluate the system performance, we construct the multicast QoE model, consisting of rebuffering time, video quality, and quality variation, which considers the mutual influence of multicast segment buffering. The specific analysis is presented as follows.

In each time slot, since each SMG can occupy the total bandwidth and computing resources in its scheduling slot, we further divide a scheduling slot into multiple mini-slots, where each SMG can occupy the total bandwidth and computing resources in its mini-slot. We define the variable $\beta_{g,t}$ as the division ratio for SMG g in scheduling slot t , which need to satisfy the following constraint, i.e.,

$$\sum_{g=1}^G \beta_{g,t} \leq 1, \forall t \in \mathcal{T}. \quad (9)$$

where \mathcal{T} is the scheduling slot set. For the simplification of expression, we omit t in the following section. Since the lagging SMG can receive segments from the leading SMG in its mini-slot, the transmission delay of leading SMG needs to consider users' channel conditions of itself and its previous SMGs. Correspondingly, the multicast transmission delay, D_g , is derived by

$$D_g = \frac{\sum_{l=1}^L \sum_{m \in \Omega_g} a_{g,m}^l \sum_{j=1}^l z_{g,m}^j}{\min_{k \in \bigcup_{d=1}^g \mathcal{K}_d} \beta_g r_{g,k}}. \quad (10)$$

Since each segment can have multiple layers that correspond to different versions, we define a binary version selection variable $a_{g,m}^l$, where $a_{g,m}^l = 1$ indicates segment layer l of video m is selected for buffering in SMG g , otherwise, $a_{g,m}^l = 0$.

To avoid repeated video transmission, we assume that only one segment version can be selected for buffering in SMG g in each time slot, which can be expressed as

$$\sum_{l=1}^L a_{g,m}^l = 1, \forall m \in \Omega_g. \quad (11)$$

Since the transmission process and transcoding process can be conducted in parallel, the service delay of SMG g can be expressed as

$$S_g = \max \left\{ D_g, \frac{\mu \sum_{l=1}^L \sum_{m \in \Omega_g} a_{g,m}^l \sum_{j=1}^l z_{g,m}^j}{\beta_g C} \right\}. \quad (12)$$

Based on SMG g 's current actual buffer 0 and service delay, we refer to [6] to derive the rebuffering time, i.e.,

$$R_g = [S_g - \tilde{q}_g^0]^+. \quad (13)$$

SSIM is a common metric used in video quality assessment. The relationship between video bitrate, b , and SSIM, Q , can be depicted as $Q = 1 - \frac{1}{2b+1}$ [30], where Q ranges from 0 to 1 and a higher Q means a higher video quality. Based on this mathematical relationship, the video quality of new buffered segments in SMG g can be expressed as

$$Q_g = \sum_{m \in \Omega_g} 1 - \frac{1}{2 \sum_{l=1}^L a_{g,m}^l \sum_{j=1}^l z_{g,m}^j / \tau + 1}. \quad (14)$$

Based on video quality, we can analyze the video quality variation, V_g , between adjacent segments in SMG g , depicted by

$$V_g = \frac{1}{|\Omega_g|} \sum_{m=1}^{|\Omega_g|} |Q_{g,m} - Q_{g,m-1}|. \quad (15)$$

where $Q_{g,0}$ is the video quality of the last segment in SMG g 's buffer before new segment buffering.

To reflect the user's satisfaction with network management, three factors including rebuffering time, video quality, and quality variation, can be integrated into the multicast QoE model, as referred in [31], which can be expressed as

$$\Upsilon_g(\mathbf{a}_g, \beta_g) = Q_g - \lambda_{g,1} R_g - \lambda_{g,2} V_g, \quad (16)$$

where \mathbf{a}_g is a vector whose unit element is $a_{g,m}^l$. Here, $\lambda_{g,1}$ and $\lambda_{g,2}$ represent users' sensitivity degrees of rebuffering time and quality variation in SMG g , respectively.

Considering each SMG has multiple segments to be buffered with different buffering orders, we need to incorporate the impact of buffering order into resource allocation. Therefore, we transform the buffering order into weighting factors, which can be expressed as

$$\omega_g = \frac{\sum_{m=1}^{\Omega_g} \phi_{g,m}}{\sum_{g=1}^G \sum_{m=1}^{\Omega_g} \phi_{g,m}}, \quad (17)$$

where $\phi_{g,m}$ is the buffering order of segment m for SMG g , and a larger value corresponds to a higher buffering priority. Based on weighting factors, we can refine the established QoE model, i.e.,

$$\tilde{\Upsilon}_g = \omega_g \Upsilon_g. \quad (18)$$

VI. PROBLEM FORMULATION AND SOLUTION

A. Problem Formulation

Since each SMG's bandwidth and computing resource demands are dynamic due to users' dynamic swipe behaviors and video requests, the reserved bandwidth and computing resources need to be flexibly and accurately allocated to each SMG at each scheduling slot to reduce playback lags. Furthermore, the versions of segments to be buffered need to be as high and stable as possible to ensure high video playback quality. By achieving low playback lags and high video playback quality, users can obtain better QoE. Based on the above analysis, our objective is to maximize users' long-term QoE by optimizing segment version selection and slot division at each scheduling slot. The formulated problem **P1** is given by

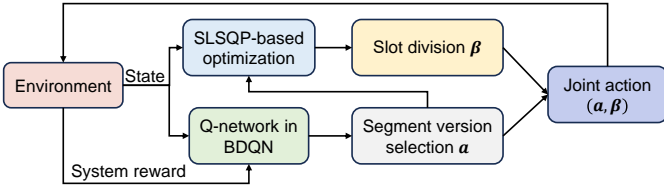


Fig. 6. The proposed data-model-driven algorithm structure.

$$\mathbf{P1} : \max_{\{\mathbf{a}_{g,t}, \beta_{g,t}\}_{t \in \mathcal{T}}} \frac{1}{T} \sum_{t=1}^T \sum_{g \in \mathcal{G}} \tilde{\Upsilon}_g(\mathbf{a}_{g,t}, \beta_{g,t}) \quad (19)$$

s.t. (9) and (11),

$$a_{g,m,t}^l \in \{0, 1\}, \forall g \in \mathcal{G}, m \in \Omega_g, l \in \mathcal{L}, t \in \mathcal{T}, \quad (19a)$$

$$\beta_{g,t} \in [0, 1], \forall g \in \mathcal{G}, t \in \mathcal{T}. \quad (19b)$$

Constraint (9) is the resource capacity constraint, which guarantees that the total scheduled bandwidths and computing resources cannot exceed the system capacity. Constraint (11) is the video transmission constraint, which avoids the repeated video transmission for each SMG.

B. Solution

We omit t in this subsection for the simplification of expression. The formulated problem is a mixed-integer nonlinear programming problem with the objective of maximizing users' long-term QoE. The dimension of \mathbf{a} is $2^L \sum_{g \in \mathcal{G}} g^{|\Omega_g|}$, which is very huge when the numbers of SMGs, recommended segments, and segment versions are high. The variable vector β are continuous values ranging from 0 to 1. Since these variables are coupled with each other, it is hard to directly use a data-driven or model-based method to solve it [32], [33]. Therefore, we consider a data-model-driven algorithm to solve it, as shown in Fig. 6. The state from the environment is first input into Q-network in the branching dueling Q network (BDQN) [34] to solve the high dimension of variable \mathbf{a} . Based on the segment version selection, we then utilize the sequential least squares quadratic programming (SLSQP) algorithm to obtain the optimal β . Finally, the joint action $\{\mathbf{a}, \beta\}$ is fed back to the environment to obtain the system reward, which is utilized for Q-network update. The detailed procedure is presented as follows.

1) *DRL-Based Segment Version Selection*: To solve the segment version selection optimization subproblem, we employ the BDQN algorithm, whose architecture is shown in Fig. 7.

As shown in Fig. 7, SMGs' state consisting of buffer lengths, channel gains, and video quality, i.e., $s = \left\{ \left\{ \tilde{q}_g^0 \right\}_{g \in \mathcal{G}}, \left\{ h_{g,k} \right\}_{k \in \mathcal{K}_g, g \in \mathcal{G}}, \left\{ Q_{g,0} \right\}_{g \in \mathcal{G}} \right\}$, are concatenated and input into the fully connected neural networks. The BDQN architecture is an amalgamation of Dueling Q-Networks [35] and a branching action mechanism, which comprises two key components, i.e., value function and advantage function. The value function $V(s)$ estimates the value of being in a particular state, independent of any specific action. Advantage function A_g exists in each action branch g , which estimates the additional value of taking a particular action in a given

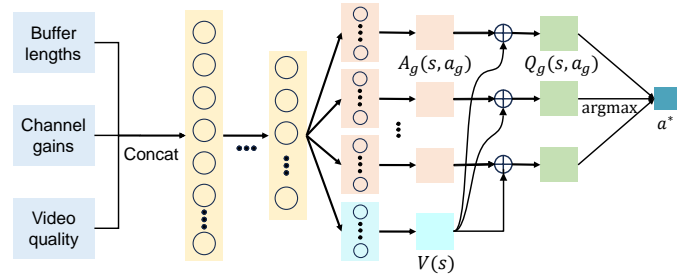


Fig. 7. The constructed BDQN architecture.

state, relative to other actions. The segment version selection decision is split into G sub-actions, where the sub-action for SMG g is denoted by $\mathbf{a}_g = \{a_{g,m}^l\}_{m \in \Omega_g, l \in \mathcal{L}}$. Each action branch corresponds to a SMG. The reward function is SMGs' QoE, i.e., $\sum_{g \in \mathcal{G}} \tilde{\Upsilon}_g(\mathbf{a}_g, \beta_g)$. The advantage function of each sub-action, i.e., $A_g(s, \mathbf{a}_g)$ is trained with the common state value $V(s)$ by experience replay. The Q-value of each sub-action is updated based on the average advantage functions, which can be expressed as

$$Q_g(s, \mathbf{a}_g) = V(s) + \left(A_g(s, \mathbf{a}_g) - \frac{1}{\rho_g} \sum_{\mathbf{a}'_g \in A_g} A_g(s, \mathbf{a}'_g) \right), \quad (20)$$

where \mathbf{a}'_g is the next-step sub-action for SMG g and ρ_g is the sub-action dimension, i.e., $2 \times \|\Omega_g\| \times L$. In each step, BDQN has a probability, i.e., $(1 - \zeta)$, to select the action that can obtain the highest Q-value, which can be expressed as

$$\mathbf{a} = \left\{ \arg \max_{\mathbf{a}'_1} Q_1(s, \mathbf{a}'_1; \boldsymbol{\theta}_1), \dots, \arg \max_{\mathbf{a}'_G} Q_G(s, \mathbf{a}'_G; \boldsymbol{\theta}_G) \right\}, \quad (21)$$

where $\boldsymbol{\theta}_g$ is the network weights of Q-network g .

To enable the agent to efficiently train, we employ the temporal-difference (TD) target after every step, which is an estimate of the expected return (future cumulative reward) for a given state-action pair, expressed by

$$y = r + \vartheta \frac{1}{G} \sum_g \hat{Q}_g \left(s', \arg \max_{\mathbf{a}'_g} Q_g(s', \mathbf{a}'_g) \right). \quad (22)$$

To quantify the difference between the predicted and target Q-values, a loss function is essential, which can guide the optimization of neural network parameters to improve learning accuracy. The loss is the expected value of mean square error across the branches, i.e.,

$$L(\boldsymbol{\theta}) = \mathbb{E}_{(s, \mathbf{a}, r, s') \sim \mathcal{D}} \left[\frac{1}{G} \sum_g (y - Q_g(s, \mathbf{a}_g))^2 \right]. \quad (23)$$

Furthermore, the prioritization error is crucial for efficiently focusing the learning process on the most informative experiences, by prioritizing those with higher TD errors in the training process. Here, the prioritization error is defined by summing across a transition's absolute, i.e.,

$$\delta_{\mathcal{D}}(s, \mathbf{a}, r, s') = \sum_g |y_g - Q_g(s, \mathbf{a}_g)|. \quad (24)$$

Algorithm 1: BDQN-based segment version selection

```

1 Input: SMGs' buffer lengths  $\tilde{q}$ , channel gains  $h$ ,
   video quality  $Q$ , and network update threshold  $\Gamma$ ;
2 Output: Segment version selection  $\mathbf{a}$ ;
3 Initialize: Replay memory  $\mathcal{D}$ , action-value function  $\mathbb{Q}$ 
   with random weights  $\theta$ , target action-value function
    $\hat{\mathbb{Q}}$  with weights  $\theta'$ ;
4 for each episode do
5   Reset initial state  $s_1$ ;
6   for each step  $t \in \{1, \dots, T\}$  do
7     With probability  $\zeta$  select a random action  $\mathbf{a}_t$ ,
       otherwise, the action is selected based on
       Eq. (21);
8     Implement the Algorithm 2 to obtain slot
       division  $\beta_t$ ;
9     Execute joint action  $(\mathbf{a}_t, \beta_t)$  in the
       environment;
10    Observe reward  $r_t$  and new state  $s_{t+1}$ ;
11    Store transition  $(s_t, \mathbf{a}_t, r_t, s_{t+1})$  in  $\mathcal{D}$ ;
12    Prioritize replay based on Eq. (24) to obtain a
       transition  $(s_j, \mathbf{a}_j, r_j, s_{j+1})$  from  $\mathcal{D}$ ;
13    Calculate the TD target based on Eq. (22);
14    Perform a gradient descent step based on the
       loss in Eq. (23);
15    Every  $\Gamma$  steps, reset  $\hat{\mathbb{Q}} = \mathbb{Q}$ ;
16  end
17 end

```

Based on the above analysis, the detailed algorithm procedure to determine segment version selection variable \mathbf{a} is shown in Algorithm 1.

2) *Optimization-Based Slot Division:* We first transform the maximization problem into the minimization problem. When \mathbf{a} is determined, denoted by \mathbf{a}^* , the original objective function in the maximization problem can be transformed to the opposite objective function in the minimization problem, i.e., $\sum_{g \in \mathcal{G}} \hat{\Upsilon}_g(\mathbf{a}_g^*, \beta_g) = -\sum_{g \in \mathcal{G}} \tilde{\Upsilon}_g(\mathbf{a}_g^*, \beta_g)$.

Theorem 1: The transformed objective function $\sum_{g \in \mathcal{G}} \hat{\Upsilon}_g(\mathbf{a}_g^*, \beta_g)$ is convex about β .

Proof: See Appendix A. ■

For the transformed convex problem, we need to find an effective algorithm to solve it. SLSQP is adept at solving the formulated linear constrained convex optimization problem by iteratively approximating them into quadratic subproblems [36]. The algorithm can converge to a global minimum for a convex problem due to the following reasons. First, by leveraging the gradient information and incorporating the constraints into Lagrange multipliers, SLSQP ensures that the solution not only optimizes the objective function but also strictly adheres to the problem's constraints. Second, given that our decision variables are continuous and bounded, SLSQP's design inherently aligns with the problem's structure, making it reliable to find the optimal solution. SLSQP needs the gradient information, but the optimization problem is not derivative at every point. Therefore, we employ the sub-gradient method [37] to analyze its sub-gradient.

Algorithm 2: SLSQP-based slot division

```

1 Input: Segment version selection  $\mathbf{a}$ , video bitrate
   sequence  $\mathbf{z}$ , bandwidth  $B$ , computing capacity  $C$ ,
   downlink transmission power  $P^{\text{DL}}$ , noise power  $N_0$ ,
   and buffer length  $\tilde{q}$ ;
2 Output: Optimal slot division  $\beta^*$ ;
3 Initialize:  $i = 0$ ,  $\beta^{(i)} = \beta^{(0)}$ , converge = False;
4 while converge == False do
5   Calculate the gradient  $\nabla \hat{\Upsilon}(\beta^{(i)})$ ;
6   Approximate the objective function and constraints
   at  $(\mathbf{a}^*, \beta^{(i)})$  by quadratic functions;
7   Formulate the quadratic subproblem P2;
8   Solve the quadratic subproblem to get direction
    $\mathbf{d}^{(i)}$ ;
9   Update the solution using a line search:
    $\beta^{(i+1)} = \beta^{(i)} + \alpha \cdot \mathbf{d}^{(i)}$ ;
10  if  $\|\beta^{(i+1)} - \beta^{(i)}\| < \varepsilon$  then
11    converge = True;
12  end
13  Increase the iteration number,  $i \leftarrow i + 1$ ;
14 end
15 Return  $\beta^* = \beta^{(i)}$ ;

```

In iteration i , the sub-gradient of $\hat{\Upsilon}_g(\mathbf{a}_g^*, \beta_g^{(i)})$ can be determined based on the value of $(x)^+$ function. Let denote $\hat{\Upsilon}_g(\mathbf{a}_g^*, \beta_g^{(i)}) = \frac{1}{\beta_g^{(i)}} \varphi_{g,1} - \varphi_{g,2}$, where functions $\varphi_{g,1}$ and $\varphi_{g,2}$ can be expressed as $\varphi_{g,1} = \omega_g \lambda_{g,1} \max\{\Xi_1(\beta_g), \Xi_2(\beta_g)\}$ and $\varphi_{g,2} = \tilde{q}_g^0(\mathbf{a}_g^*)$. Functions $\varphi_{g,1}$ and $\varphi_{g,2}$ are constants related with \mathbf{a}_g^* . In addition, functions $\Xi_1(\beta_g)$ and $\Xi_2(\beta_g)$ are defined in Appendix A.

Then, we can have the sub-gradient of variable for slot division variable $\beta_g^{(i)}$:

$$\nabla \hat{\Upsilon}(\beta_g^{(i)}) = \begin{cases} -\frac{\varphi_{g,1}}{(\beta_g^{(i)})^2}, & \beta_g^{(i)} < \frac{\varphi_{g,1}}{\varphi_{g,2}}, \\ -\sigma \frac{\varphi_{g,1}}{(\beta_g^{(i)})^2}, & \beta_g^{(i)} = \frac{\varphi_{g,1}}{\varphi_{g,2}}, \\ 0, & \text{otherwise,} \end{cases} \quad (25)$$

where σ is a positive value with the range of $(0, 1]$.

Based on the sub-gradient information, the Hessian matrix, \mathbf{H} , is expressed as $\text{diag}(\nabla^2 \hat{\Upsilon}(\beta_1^{(i)}), \dots, \nabla^2 \hat{\Upsilon}(\beta_G^{(i)}))$. Since the quadratic subproblem is a fundamental step in the SLSQP algorithm, we formulate the quadratic subproblem as

$$\mathbf{P2:} \min_{\beta^{(i)}} \hat{\Upsilon}(\mathbf{a}^*, \beta^{(i)}) + \nabla \hat{\Upsilon}(\mathbf{a}^*, \beta^{(i)})^T \mathbf{d} + \frac{1}{2} \mathbf{d}^T \mathbf{H} \mathbf{d} \quad (26)$$

$$\text{s.t. } c(\beta^{(i)}) + \nabla c(\beta^{(i)})^T \mathbf{d} \leq 0, \quad (26a)$$

$$\beta^{(i)} + \mathbf{d} \in [0, 1], \quad (26b)$$

where the objective function is the quadratic approximation around $(\mathbf{a}^*, \beta^{(i)})$. Here, c and \mathbf{d} represent the function of Eq. (9) and the direction of change, respectively.

To solve the formulated quadratic subproblem, we can utilize the QP solver in the CVXOPT¹. The specific algorithm

¹CVXOPT: <https://cvxopt.org/examples/tutorial/qp.html>

TABLE I
SIMULATION PARAMETERS

Parameter	Value	Parameter	Value
B	[6, 14] MHz	K	[10, 26]
C	[8, 12] Gcycles/s	μ	4 Gcycles/Mb
T_s	5 sec	λ_1	[0.2, 0.4]
τ	2 sec	λ_2	[0.5, 0.7]
P_D	27 dBm	N_0	-174 dBm

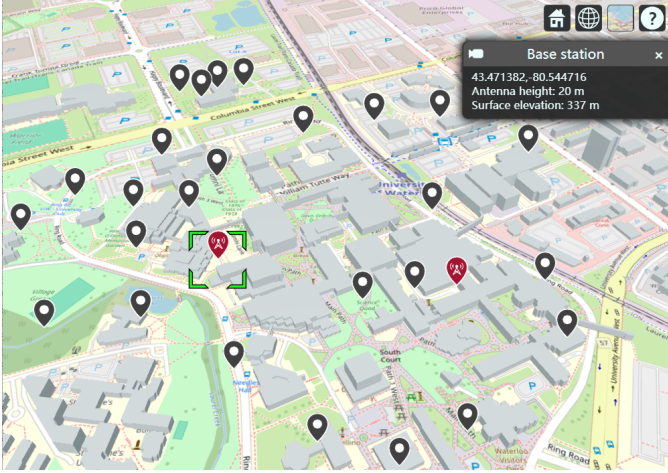


Fig. 8. The simulation scene, where BSs and users are represented by red and gray icons, respectively.

is shown in Algorithm 2.

VII. SIMULATION RESULTS

We conduct extensive simulations on the real-world dataset to evaluate the performance of the proposed DT-based network management scheme.

A. Simulation Setup

We adopt the short video streaming dataset² to obtain users' swipe behaviors. We sample 1000 short videos from the YouTube 8M dataset³, which includes 8 video types, i.e., Entertainment, Games, Food, Sports, Science, Dance, Travel, and News. Each video sequence is encoded into four versions, i.e., $L = 4$. We consider the scenario where two BSs are deployed at the University of Waterloo (UW) campus and users' initial positions are randomly and uniformly generated around two BSs, as shown in Fig. 8. Each user moves along a prescribed path within the UW campus at a speed of 2 ~ 5 km/h, and the corresponding channel path loss is obtained by the propagationModel at Matlab. The main simulation parameters are presented in Table I.

Our BDQN architecture consists of four fully connected layers, transitioning from an initial state-size input to a layer with 128 nodes. This architecture is split into two streams:

²ACM MM Grand Challenges: <https://github.com/AItransCompetition/Short-Video-Streaming-Challenge/tree/main/data>

³YouTube 8M dataset: <https://research.google.com/youtube8m/index.html>

TABLE II
BDQN PARAMETERS

Parameter	Value	Parameter	Value
Memory size	5000	Episode length	75
Initial epsilon	1	Discount factor	0.9
Epsilon decay	0.99	Learning rate	0.001
Final epsilon	0.1	Batch size	64
Number of episodes	500	NN layer connection	FC
Hidden layer structure	512 × 256 × 256 × 128	Activation function	ReLU
Advantage stream structure	128 × 36	Value stream structure	128 × 1

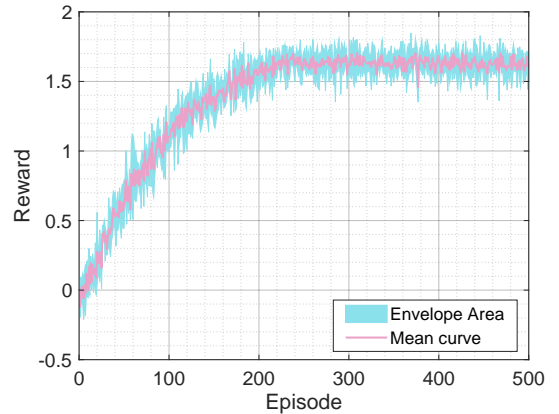


Fig. 9. Convergence performance of proposed DT-based network management scheme.

a value stream with a single output and multiple advantage streams, which can produce a matrix of action advantage values that represents the combination of actions and their respective choices. To refine the learning process, we integrate a prioritized replay buffer, which emphasizes learning from experiences with higher predicted errors. The parameter setting and model structure are presented in Table II.

We compare the proposed DT-based network management scheme with the following benchmark schemes:

- **Without DT (WDT) scheme:** The segment buffering is based on the sequential principle. The rebuffering time estimation is based on the service delay and the SMGs' currently total buffered segments. The determination of segment version selection and slot division employs the same data-model-driven method proposed in the DT-based network management scheme.
- **Heuristic scheme [5]:** The segment buffering and buffer update employ the same principle proposed in the DT-based network management scheme. The scheduling slot is discretized into 10 mini-slots. Each mini-slot is first provisionally allocated to each SMG, and then the corresponding segment version selection is determined by the branch and bound algorithm. Finally, the mini-slot is ultimately allocated to the SMG that can obtain the maximum QoE.

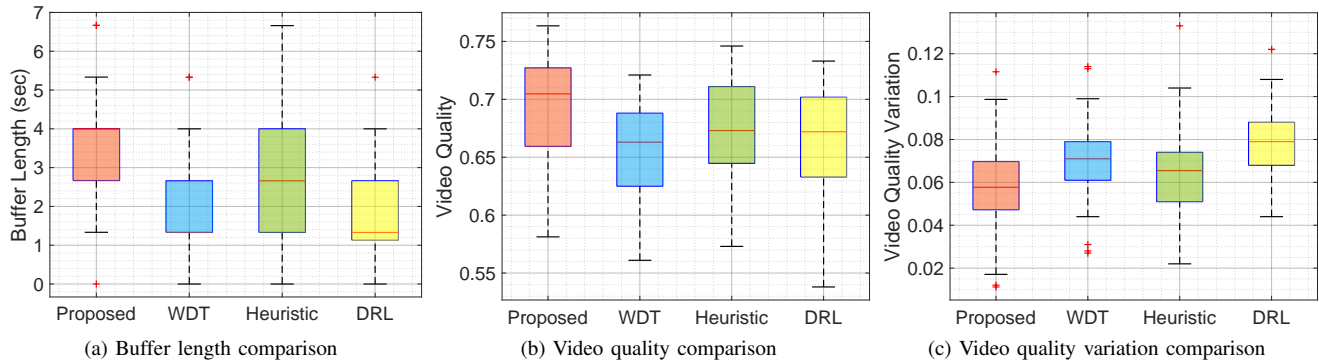


Fig. 10. The performance comparison of different QoE components.

- DRL-based scheme:** The segment buffering is based on the sequential principle. The rebuffering time estimation is based on the service delay and the SMGs' currently total buffered segments. The joint optimization of segment version selection and slot division is determined by the modified DDPG algorithm [38], where the range of segment version selection action is divided into four parts, i.e., $[0, 0.25)$, $[0.25, 0.5)$, $[0.5, 0.75)$, $[0.75, 1]$, corresponding to the segment version from low to high. Furthermore, a hierarchical reward is used to accelerate the algorithm's training speed.

B. Convergence Analysis

In this subsection, we analyze the convergence performance of the proposed scheme within 500 training episodes. As shown in Fig. 9, we present the convergence curve of the DT-based network management scheme. We conducted four training trials to draw the corresponding envelope area and mean curve, where each training trail corresponds to a unique seed for action exploration and experience replay. Each episode consists of 75 steps, and the corresponding reward is the average reward for all steps within an episode. It can be observed that as the number of episodes increases, the reward gradually grows larger. When the number of episodes approaches nearly 230, the reward converges to a stable state, indicating that the DT-based network management scheme can achieve a high and stable QoE for users.

C. Performance Evaluation of QoE Components

In this subsection, we evaluate the performance of the MG's QoE components. The bandwidth, computing capacity, and user number are set to 10 MHz, 10 Gcycles/s, and 10 respectively. We present the box plot comparison of buffer length, video quality, and video quality variation across four different schemes in Fig. 10. Each box plot delineates the interquartile range, median, and outliers.

As shown in Fig. 10(a), the proposed scheme demonstrates a higher median buffer length and a more compact interquartile range relative to the other schemes, which indicates users' equipment can buffer more segments to reduce the rebuffering probability. The compactness of the proposed scheme suggests lower variability in buffer length, which could bring

a more stable user experience during video playback. The reason that the proposed scheme can achieve a better buffer length performance is attributed to the proposed DT-assisted segment buffer scheme, which can effectively abstract the watching probability distribution for priority-based buffering and maintain multiple virtual buffers for accurate buffer length updates.

Fig. 10(b) presents a comparative analysis of video quality performance among different schemes with the range from 0.53 to 0.77. The proposed scheme reveals the highest median video quality, as well as a relatively narrower interquartile range compared to the other schemes. This suggests that the proposed scheme not only delivers a relatively higher video quality but also ensures smoother playback in the quality of streaming content. The reduced spread of data points and fewer outliers underscores its ability to provide a reliably high-quality watching experience, due to its advanced segment version selection algorithm that can achieve a good trade-off between buffering and streaming quality.

As shown in Fig. 10(c), we present the comparison of video quality variation. Based on the observation, the proposed scheme shows the lowest median value that suggests a central tendency towards lower variation in video quality. Despite the interquartile range of the proposed scheme being very close to the other schemes, the concentration of data around a lower median value and the reduced number of extreme outliers reflect its effectiveness in ensuring stable video quality.

D. Performance Evaluation of QoE Under Different Settings

We present QoE comparison under different users, bandwidths, and computing capacities among different schemes in Fig. 11. Overall, the proposed scheme can achieve superior performance under different simulation settings.

Fig. 11(a) describes the correlation between the number of users and QoE. Based on the observation, we find that QoE initially increases and then decreases as the number of users increases due to the mutual influence of multicast segment buffering. Specifically, the increased users can lead to more users being clustered into one SMG and enrich users' diversity. Initially, the same multicast segments watched by the original users may gain a better QoE for newly clustered users who have low sensitivity degrees. However, with the

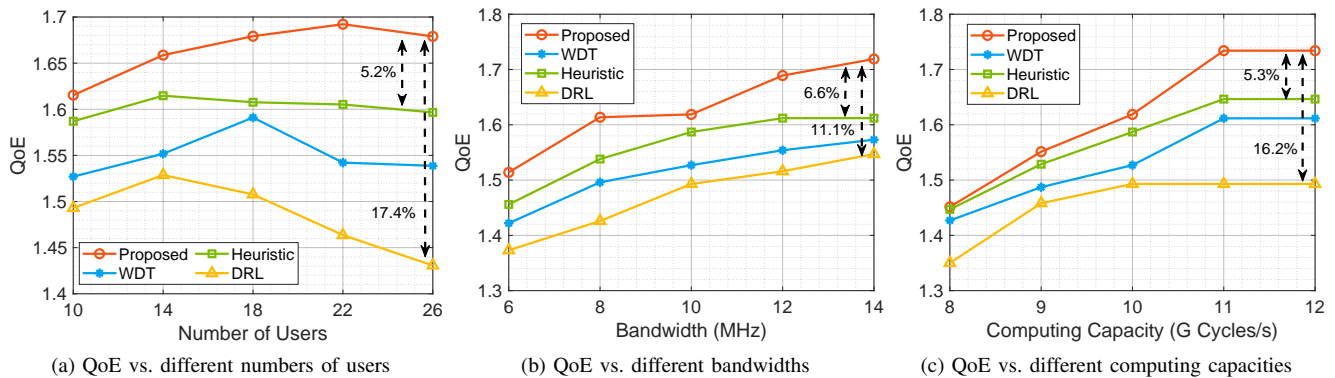
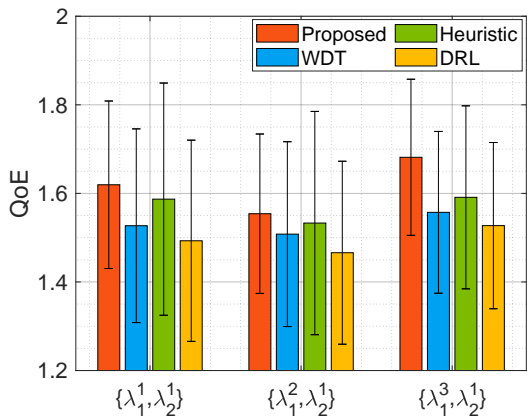
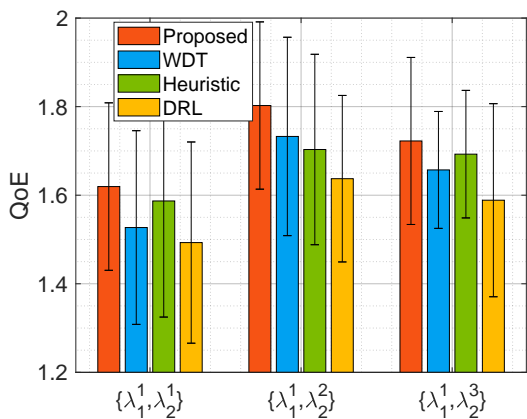


Fig. 11. QoE comparison under different users, bandwidths, and computing capacities.



(a) QoE vs. different sensitivity degrees of rebuffering time



(b) QoE vs. different sensitivity degrees of video quality variation

Fig. 12. QoE comparison under different sensitivity degrees.

increased number of users, the multicast segments cannot always satisfy users' differentiated watching requirements, which finally leads to low QoE. The proposed scheme exhibits a QoE of approximately 1.68 when catering to 26 users, a 5.2% and 17.4% increase compared to the heuristic and DRL schemes, which demonstrates the effectiveness of the proposed scheme.

Fig. 11(b) presents the QoE variation with the increased bandwidth. The proposed scheme's upward tendency in

QoE with increased bandwidth implies that it can well adapt to varying network capacities, which is essential for ensuring service quality during peak usage times or in bandwidth-constrained environments. When the bandwidth reaches 14 MHz, the proposed scheme achieves a QoE increment of 11.1% compared to the DRL scheme, suggesting that the proposed scheme can efficiently utilize available bandwidth to enhance the user experience.

Fig. 11(c) correlates the computing capacity with QoE. In MSVS, the computing capacity directly influences the transcoding version and the speed for segments to be delivered to SMGs. The proposed scheme's pronounced improvement in QoE with the increasing computing capacity reflects its ability to leverage additional computational resources effectively for video transcoding management. Here, the proposed scheme reached a QoE of around 1.75 with a computing capacity of 12 Gcycles/s, which is a significant 16.2% improvement over the DRL method. This suggests that the proposed scheme can effectively harness computing power to enhance video quality for QoE improvement.

Furthermore, we present the QoE comparison under different sensitivity degrees among different schemes in Fig. 12. As shown in Fig. 12(a), we adjust the SMGs's sensitivity degrees of video rebuffering time with the fixed sensitivity degrees of video quality variation. The parameter λ_1^1 includes three elements, i.e., (0.4, 0.3, 0.2), which represents three SMGs' sensitivity degrees of rebuffering time, respectively. The parameter λ_2^1 also includes three elements, i.e., (0.7, 0.6, 0.5). While the parameters λ_1^2 and λ_1^3 are set to (0.3, 0.3, 0.3) and (0.2, 0.3, 0.4), respectively. Different settings of sensitivity degrees of rebuffering time aim at validating the effectiveness of the proposed scheme in the diversified SMGs. It can be observed that our proposed scheme can always achieve the highest QoE with a comparatively tighter range of variance under different parameters λ_1 . As shown in Fig. 12(b), we change the SMGs' sensitivity degrees of video quality variation with the fixed sensitivity degrees of rebuffering time. The parameters λ_2^2 and λ_2^3 are set to (0.6, 0.6, 0.6) and (0.5, 0.6, 0.7), respectively. Compared with the first error bar, the last two error bars obtain higher QoE values with similar variance. This is because the last two SMGs are much more sensitive to video quality variation and they need

$$\widehat{\Upsilon}_g(a_g^*, \beta_g) = \omega_g \left(\sum_{m \in \Omega_g} -1 + \frac{1}{2a_{g,m}^{l^*} \sum_{j=1}^{l^*} z_{g,m}^j / \tau + 1} + \frac{\lambda_{g,2}}{|\Omega_g|} \sum_{m \in \Omega_g} \left| Q_{g,m}^{l^*}(a_{g,m}^*) - Q_{g,m-1}^{l^*}(a_{g,m-1}^*) \right| \right) + \omega_g \lambda_{g,1} \left[\max \left\{ \frac{\sum_{m \in \Omega_g} a_{g,m}^{l^*} \sum_{j=1}^{l^*} z_{g,m}^j}{\min_{k \in \bigcup_{d=1}^g \mathcal{K}_d} \beta_g B \log_2 \left(1 + \frac{|h_{g,k}|^2 P_D}{N_0} \right)}, \frac{\mu \sum_{m \in \Omega_g} a_{g,m}^{l^*} \sum_{j=1}^{l^*} z_{g,m}^j}{\beta_g C} \right\} - \widetilde{q}_g^0 \right]^+. \quad (27)$$

to be allocated more bandwidth and computing resources to guarantee their smooth and high-quality video playback. Therefore, with a higher weighting factor, SMGs' QoE can be effectively enhanced.

VIII. CONCLUSION

In this paper, we have proposed a novel DT-based network management scheme to enhance QoE in MSVS. Furthermore, we have established a multicast QoE model to quantify the impact of multicast segment buffering among SMGs. A convex optimization embedded DRL algorithm has been designed to determine the joint segment version selection and slot division. The proposed DT-based network management scheme can efficiently multicast segment buffering in MSVS. For the future work, we will investigate the adaptive granularity of DT data collection and abstraction to reduce the network overhead of DT.

APPENDIX A PROOF OF THEOREM 1

When the variable \mathbf{a} is determined, the opposite objective function in the minimization problem can be expressed in Eq. (27).

Let denote

$$\Xi_1(\beta_g) = \left\{ \frac{\sum_{m \in \Omega_g} a_{g,m}^{l^*} \sum_{j=1}^{l^*} z_{g,m}^j}{\min_{k \in \bigcup_{d=1}^g \mathcal{K}_d} \beta_g B \log_2 \left(1 + \frac{|h_{g,k}|^2 P_D}{N_0} \right)} \right\}$$

and

$$\Xi_2(\beta_g) = \left\{ \frac{\mu \sum_{m \in \Omega_g} a_{g,m}^{l^*} \sum_{j=1}^{l^*} z_{g,m}^j}{\beta_g C} \right\},$$

then the last term of Eq. (27) can be transformed into

$$\omega_g \lambda_{g,1} \left(\max \left\{ [\Xi_1(\beta_g) - \widetilde{q}_g^0]^+, [\Xi_2(\beta_g) - \widetilde{q}_g^0]^+ \right\} \right).$$

Since the second derivative of functions $\Xi_1(\beta_g)$ and $\Xi_2(\beta_g)$ are positive values, i.e., $\frac{\partial^2 \Xi_1(\beta_g)}{\partial^2 \beta_g} \geq 0$, $\frac{\partial^2 \Xi_2(\beta_g)}{\partial^2 \beta_g} \geq 0$, they are convex functions. Then, we need to prove the convexity of function $\psi_1(\beta_g) = [\Xi_1(\beta_g) - \widetilde{q}_g^0]^+$ and $\psi_2(\beta_g) = [\Xi_2(\beta_g) - \widetilde{q}_g^0]^+$.

Consider an arbitrary value $\theta \in (0, 1)$, and arbitrary values $\beta_{g,1}$, and $\beta_{g,2}$, we have

$$\begin{aligned} & \psi_1(\theta \beta_{g,1} + (1 - \theta) \beta_{g,2}) \\ &= \max \{ \Xi_1(\theta \beta_{g,1} + (1 - \theta) \beta_{g,2}) - \widetilde{q}_g^0, 0 \} \\ &\leq \max \{ \theta \Xi_1(\beta_{g,1}) + (1 - \theta) \Xi_1(\beta_{g,2}) - \widetilde{q}_g^0, 0 \} \\ &\leq \theta \max \{ \Xi_1(\beta_{g,1}) - \widetilde{q}_g^0, 0 \} \\ &\quad + (1 - \theta) \max \{ \Xi_1(\beta_{g,2}) - \widetilde{q}_g^0, 0 \} \\ &= \theta \psi_1(\beta_{g,1}) + (1 - \theta) \psi_1(\beta_{g,2}). \end{aligned} \quad (28)$$

Therefore, the function $\psi_1(\beta_g)$ is convex. The same validation method can be applied to $\psi_2(\beta_g)$ and $\max \{ \psi_1(\beta_g), \psi_2(\beta_g) \}$. Therefore, the component $\omega_g \lambda_{g,1} (\max \{ \psi_1(\beta_g), \psi_2(\beta_g) \})$ is convex. Since the first two terms of the first line of Eq. (27) are constant, they do not affect the convexity of the transformed objective function. Therefore, function $\widehat{\Upsilon}_g(a_g^*, \beta_g)$ is convex. For functions $\widehat{\Upsilon}_g(a_g^*, \beta_g)$ with different g , they have an identical domain and are mutually independent with each other, so their summation is also a convex function. Based on the above analysis, the transformed objective function is convex.

REFERENCES

- [1] The Outloud Group, "Top tiktok statistics (2023): Key facts, figures, & data," 2023. [Online]. Available: <https://www.outloudgroup.com/post/top-tik-tok-statistics-demographics>
- [2] X. Jiang, F. R. Yu, T. Song, and V. C. Leung, "A survey on multi-access edge computing applied to video streaming: Some research issues and challenges," *IEEE Commun. Surv. Tut.*, vol. 23, no. 2, pp. 871–903, 2021.
- [3] X. Huang, W. Wu, S. Hu, M. Li, C. Zhou, and X. Shen, "Digital twin based user-centric resource management for multicast short video streaming," *IEEE J. Sel. Topics Signal Process.*, pp. 1–16, 2023, Early Access.
- [4] J. Nightingale, P. Salva-Garcia, A. Calero, and Q. Wang, "5G-QoE: QoE modelling for ultra-HD video streaming in 5G networks," *IEEE Trans. Broadcast.*, vol. 64, no. 2, pp. 621–634, 2018.
- [5] X. Huang, L. He, L. Wang, and F. Li, "Towards 5G: Joint optimization of video segment caching, transcoding and resource allocation for adaptive video streaming in a multi-access edge computing network," *IEEE Trans. Veh. Technol.*, vol. 70, no. 10, pp. 10909–10924, 2021.
- [6] W. Huang, Y. Zhou, X. Xie, D. Wu, M. Chen, and E. Ngai, "Buffer state is enough: Simplifying the design of QoE-aware HTTP adaptive video streaming," *IEEE Trans. Broadcast.*, vol. 64, no. 2, pp. 590–601, 2018.
- [7] S. Wang, S. Bi, and Y. Zhang, "Adaptive wireless video streaming: Joint transcoding and transmission resource allocation," *IEEE Trans. Wirel. Commun.*, vol. 21, no. 5, pp. 3208–3221, 2022.
- [8] M. Grieves, "Digital twin: manufacturing excellence through virtual factory replication," *White paper*, vol. 1, no. 2014, pp. 1–7, 2014.
- [9] X. Huang, H. Yang, S. Hu, and X. Shen, "Digital twin-driven network architecture for video streaming," *arXiv preprint arXiv:2310.19079*, 2023.

- [10] Q. Guo, F. Tang, T. Rodrigues, and N. Kato, "Five disruptive technologies in 6G to support digital twin networks," *IEEE Wirel. Commun.*, pp. 1–8, 2023, Early Access.
- [11] M. Taha, A. Canovas, J. Lloret, and A. Ali, "A QoE adaptive management system for high definition video streaming over wireless networks," *Telecommun. Syst.*, vol. 77, pp. 63–81, 2021.
- [12] H. Li, B. Li, T. T. Tran, and D. C. Sicker, "Transmission schemes for multicasting hard deadline constrained prioritized data in wireless multimedia streaming," *IEEE Trans. Wirel. Commun.*, vol. 15, no. 3, pp. 1631–1641, 2016.
- [13] L. Zhong, X. Chen, C. Xu, Y. Ma, M. Wang, Y. Zhao, and G.-M. Muntean, "A multi-user cost-efficient crowd-assisted VR content delivery solution in 5G-and-beyond heterogeneous networks," *IEEE Trans. Mobile Comput.*, vol. 22, no. 8, pp. 4405–4421, 2023.
- [14] S. Zuhra, P. Chaporkar, A. Karandikar, and P. Jha, "Leveraging multi-connectivity for multicast video streaming," *arXiv preprint arXiv:2202.05053*, 2022.
- [15] A. Daher, M. Coupechoux, P. Godlewski, P. Ngouat, and P. Minot, "A dynamic clustering algorithm for multi-point transmissions in mission-critical communications," *IEEE Trans. Wirel. Commun.*, vol. 19, no. 7, pp. 4934–4946, 2020.
- [16] M. Zhang, H. Lu, and P. Hong, "Cooperative robust video multicast in integrated terrestrial-satellite networks," *IEEE Trans. Wirel. Commun.*, vol. 21, no. 10, pp. 8276–8291, 2022.
- [17] M. Zhang, H. Lu, F. Wu, and C. Chen, "NOMA-based scalable video multicast in mobile networks with statistical channels," *IEEE Trans. Mobile Comput.*, vol. 20, no. 6, pp. 2238–2253, 2021.
- [18] E. Glaessgen and D. Stargel, "The digital twin paradigm for future NASA and U.S. air force vehicles," in *Proc. Struct. Dyn. Mater. Conf. Special Session: Digital Twin*, Honolulu, HI, USA, 2012, p. 1818.
- [19] X. Shen, J. Gao, W. Wu, M. Li, C. Zhou, and W. Zhuang, "Holistic network virtualization and pervasive network intelligence for 6G," *IEEE Commun. Surveys Tuts.*, vol. 24, no. 1, pp. 1–30, 2022.
- [20] T. Duong, D. Van, S. Khosravirad, V. Sharma, O. Dobre, and H. Shin, "From digital twin to metaverse: The role of 6G ultra-reliable and low-latency communications with multi-tier computing," *IEEE Wirel. Commun.*, vol. 30, no. 3, pp. 140–146, 2023.
- [21] A. Masaracchia, V. Sharma, B. Canberk, O. Dobre, and T. Duong, "Digital twin for 6G: Taxonomy, research challenges, and the road ahead," *IEEE Open J. Commun. Soc.*, vol. 3, pp. 2137–2150, 2022.
- [22] P. Bellavista, C. Giannelli, M. Mamei, M. Mendula, and M. Picone, "Application-driven network-aware digital twin management in industrial edge environments," *IEEE Trans. Ind. Informat.*, vol. 17, no. 11, pp. 7791–7801, 2021.
- [23] L. Qi, X. Xu, X. Wu, Q. Ni, Y. Yuan, and X. Zhang, "Digital-twin-enabled 6G mobile network video streaming using mobile crowdsourcing," *IEEE J. Sel. Areas Commun.*, vol. 41, no. 10, pp. 3161–3174, 2023.
- [24] R. Dong, C. She, W. Hardjawana, Y. Li, and B. Vucetic, "Deep learning for hybrid 5G services in mobile edge computing systems: Learn from a digital twin," *IEEE Trans. Wirel. Commun.*, vol. 18, no. 10, pp. 4692–4707, 2019.
- [25] X. Huang, W. Wu, and X. Shen, "Digital twin-assisted resource demand prediction for multicast short video streaming," in *Proc. IEEE Int. Conf. Distrib. Comput. Syst. (ICDCS)*, Hong Kong, China, 2023, pp. 967–968.
- [26] Q. Guo, F. Tang, and N. Kato, "Resource allocation for aerial assisted digital twin edge mobile network," *IEEE J. Sel. Areas Commun.*, vol. 41, no. 10, pp. 3070–3079, 2023.
- [27] S. Jeremiah, L. Yang, and J. Park, "Digital twin-assisted resource allocation framework based on edge collaboration for vehicular edge computing," *Future Gener. Comp. Sy.*, vol. 150, pp. 243–254, 2024.
- [28] Z. Li, Y. Xie, R. Netravali, and K. Jamieson, "Dashlet: Taming swipe uncertainty for robust short video streaming," in *Proc. USENIX Symp. Networked Syst. Design Implement. (NSDI)*, Boston, MA, 2023, pp. 1583–1599.
- [29] M. Wien, H. Schwarz, and T. Oelbaum, "Performance analysis of SVC," *IEEE Trans. Circuits Syst. Video Technol.*, vol. 17, no. 9, pp. 1194–1203, 2007.
- [30] G. Huang, W. Gong, B. Zhang, C. Li, and C. Li, "An online buffer-aware resource allocation algorithm for multiuser mobile video streaming," *IEEE Trans. Vehi. Technol.*, vol. 69, no. 3, pp. 3357–3369, 2020.
- [31] C. Zhou, Y. Ban, Y. Zhao, L. Guo, and B. Yu, "PDAS: Probability-driven adaptive streaming for short video," in *Proc. ACM Int. Conf. Multimedia (ACM MM)*, Lisboa, Portugal, 2022, pp. 7021–7025.
- [32] B. He, J. Wang, Q. Qi, Q. Ye, Q. Li, J. Liao, and X. Shen, "ShuttleBus: Dense packet assembling with QUIC stream multiplexing for massive IoT," *IEEE Trans. Mobile Comput.*, pp. 1–16, 2023, Early Access.
- [33] W. Jiang, B. Ai, M. Li, W. Wu, and X. Shen, "Average age-of-information minimization in aerial IRS-assisted data delivery," *IEEE Internet Things J.*, vol. 10, no. 17, pp. 15 133–15 146, 2023.
- [34] A. Tavakoli, F. Pardo, and P. Kormushev, "Action branching architectures for deep reinforcement learning," in *Proc. AAAI Conf. Artif. Intell. (AAAI)*, vol. 32, no. 1, New Orleans, Louisiana, USA, 2018, pp. 4131–4138.
- [35] Z. Wang, T. Schaul, M. Hessel, H. Hasselt, M. Lanctot, and N. Freitas, "Dueling network architectures for deep reinforcement learning," in *Proc. Int. Conf. Mach. Learn. (ICML)*, New York, NY, USA, 2016, pp. 1995–2003.
- [36] D. Kraft, "A software package for sequential quadratic programming," *Forschungsbericht- DFVLR*, 1988. [Online]. Available: http://degenerateconic.com/uploads/2018/03/DFVLR_FB_88_28.pdf
- [37] S. Boyd, L. Xiao, and A. Mutapcic, "Subgradient methods," *lecture notes of EE392o, Stanford University, Autumn Quarter*, vol. 2004, pp. 2004–2005, 2003.
- [38] T. Zhao, F. Li, and L. He, "DRL-based joint resource allocation and device orchestration for hierarchical federated learning in NOMA-enabled industrial IoT," *IEEE Trans. Ind. Informat.*, vol. 19, no. 6, pp. 7468–7479, 2023.